Chemical Science

ROYAL SOCIETY OF CHEMISTRY

EDGE ARTICLE

View Article Online
View Journal | View Issue

Cite this: *Chem. Sci.*, 2022, **13**, 8642

All publication charges for this article have been paid for by the Royal Society of Chemistry

Received 23rd April 2022
Accepted 4th July 2022

DOI: 10.1039/d2sc02308c

rsc.li/chemical-science

Caged bulky organic dyes in a polyaromatic framework and their spectroscopic peculiarities†

Mayuko Ueda, Natsuki Kishida, Lorenzo Catti and Michito Yoshizawa *

Host–guest structures and properties have been widely studied using relatively small dyes (<1 nm) without bulky groups, due to their smooth incorporation, efficient host–guest interactions, and high analytical accessibility. In this report, on the other hand, three types of sterically demanding organic dyes trapped by a polyaromatic cage were investigated by spectroscopic analyses on the basis of supramolecular interactions. Coumarins with two bulky substituents are bound by the cage in aqueous solution. The resultant caged dyes show unusual emission enhancement, depending on the difference of a single heteroatom in their substituents. The color of perylene bisimides with two bulky substituents is remarkably changed from yellow to red upon caging. This peculiarity stems from the twist of the substituents in the cage, revealed by the combination of absorption and theoretical studies. Furthermore, tetrasubstituted, bulky porphyrins are caught by the cage in aqueous solution. The caged bulky dyes also display altered color and absorption properties, which remain intact even under acidic conditions. In contrast to typical covalent functionalization and previous host–guest studies toward small and non-bulky dyes, the unusual, non-covalent spectroscopic modulation of the large and bulky dyes can be accomplished for the first time by the present cage, featuring a prolate polyaromatic framework with four openings.

Introduction

Organic dyes displaying characteristic colors are ubiquitous in our daily lives.[1] The majority of these dyes possess relatively bulky substituents and rigid core frameworks bearing extended π-conjugation systems.[2] Modulation and alteration of their colors and spectroscopic properties have been widely demonstrated by *covalent* functionalization of the frameworks as a common synthetic approach. *Non-covalent* functionalization of dyes upon encapsulation by molecular cages has recently been regarded as an alternative approach,[3] without multistep and time-consuming synthetic protocols. Coordination-driven self-assembly is one of the most promising methods for the preparation of the desired cages, from the viewpoints of high designability and synthetic accessibility.[4] However, coordination capsules and cages capable of binding such large and bulky dyes have been rarely reported so far (Fig. 1a, left), owing to size/shape mismatch as well as poor host–guest interactions in the cavity,[5] whereas the embedding of various dyes (*e.g.*, perylene bisimide and porphyrin) into the coordinative ligands is a well-established approach. We considered that a coordination-driven molecular cage featuring *both a large cavity and several medium-sized windows* would be a useful molecular tool to bind a variety of organic dyes with two and more bulky substituents (Fig. 1a, right). Here we report that, as a proof-of-concept, the open large cavity of M_2L_4 polyaromatic cage **1** (Fig. 1b and c) can

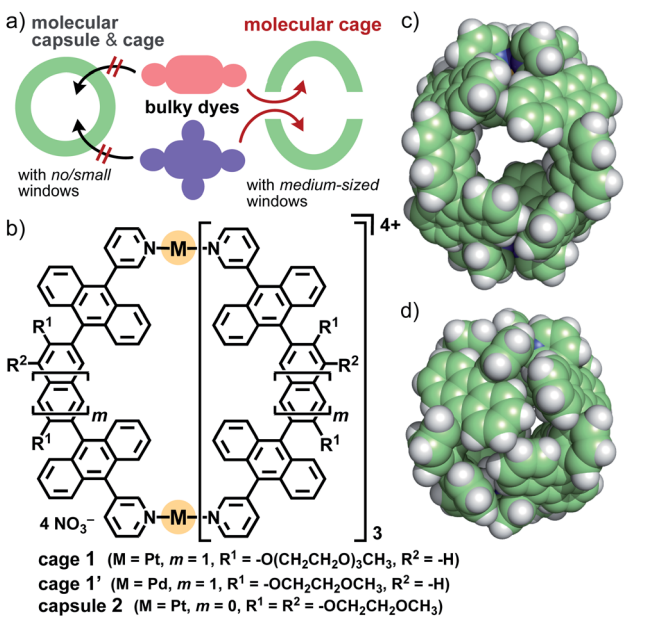

Fig. 1 (a) Strategy for the binding of bulky organic dyes by a molecular cage with medium-sized windows for their spectroscopic modulation. (b) Present aqueous cage **1**, and previous cage **1′** and capsule **2**. The crystal structures of (c) **1′** and (d) **2** ($R^1 = R^2 = H$ for clarity).[8,10]

Laboratory for Chemistry and Life Science, Institute of Innovative Research, Tokyo Institute of Technology, 4259 Nagatsuta, Midori-ku, Yokohama 226-8503, Japan. E-mail: yoshizawa.m.ac@m.titech.ac.jp

† Electronic supplementary information (ESI) available. See https://doi.org/10.1039/d2sc02308c

bind sterically demanding organic dyes (≥1.5 nm in maximum length) with (i) coumarin, (ii) perylene bisimide, and (iii) porphyrin cores in aqueous solution. Notably, the spectroscopic properties of the caged dyes are facilely modulated through effective supramolecular interactions in the cavity, without the aid of commonly employed host–guest π-stacking interactions.

Host functions of the polyaromatic cavities of coordination capsules have been highlighted recently.[6,7] For example, the *closed* polyaromatic cavity of M_2L_4 capsule **2** (Fig. 1b) shows efficient/selective binding abilities toward various synthetic compounds[8] as well as biomolecules in aqueous solution, through efficient hydrophobic effect and multipoint π–π/CH–π/hydrogen-bonding interactions.[6,9] However, like other coordination cages reported previously,[4] capsule **2** exhibits no binding ability toward synthetic dyes *with multiple bulky substituents*, whose sizes are larger than that of the cavity (d = 1.2 nm), owing to the closed spherical framework (Fig. 1d). We thus herein employed the analogous, prolate M_2L_4 cage **1′**, with a cavity size of $d_{max.}$ = 1.6 nm and a window size of $d_{max.}$ = 0.7 nm (Fig. 1c).[10] As the key molecular design in this study, the replacement of the short methoxyethoxy (MOE) side-chains with long hydrophilic ones (*i.e.*, methoxytriethylene glycol (TEG)) allows cage **1** to be used in aqueous solution as well as to bind bulky, hydrophobic organic dyes efficiently for the first time. Crystallographic insights into the host–guest structures are, on the other hand, inaccessible in this system, due to the flexibility of the side-chains.

It should be noted that, in contrast to small organic dyes, relatively large organic dyes with bulky substituents and rigid core-frameworks, studied in the present work, have several disadvantages regarding their host–guest investigations. Their low or no solubility in common solvents reduces analytical accessibility, *e.g.*, for typical Job's plot and binding constant analyses. The product yield and stability are often compromised by inefficient host–guest interactions. Accordingly, the investigations of new host–guest structures and properties using large and bulky dyes have been severely limited so far, especially in aqueous media.

Results and discussion

Synthesis of aqueous cage 1

Bispyridine ligand **3** bearing two TEG groups was synthesized from brominated, bent anthracene dimers with two MOE groups in four steps (Fig. S1–S10†).[11] TEG-substituted cage **1** was facilely formed from Pt(II) ions and ligands **3** in DMSO-d_6 (88% isolated yield), as confirmed by ^{1}H NMR and ESI-TOF MS analyses (Fig. 2a and S11–S15†).[11] The combination of DOSY, DLS, and molecular modeling studies suggested the core and outer diameters of **1** being ∼2 and ∼4 nm, respectively (Fig. 2c).[12] The multiple, long and flexible side-chains suppress its self-aggregation in solution and ordered packing in the solid state. Whereas MOE-substituted cage **1′** is insoluble in water, present cage **1** is slightly soluble in water (∼0.04 mM; Fig. S17†) and well-soluble in 15 : 1 water/acetonitrile solution at room temperature. A Pd(II) analogue, obtained in the same way, showed lower water-solubility relative to **1**. The fully-assignable,

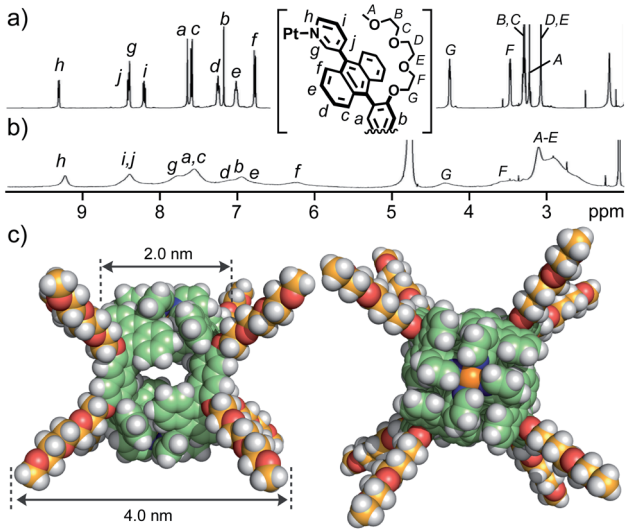

Fig. 2 ^{1}H NMR spectra (400 MHz, r.t.) of cage **1** in (a) CD_3CN and (b) 15 : 1 D_2O/CD_3CN. (c) Optimized structure of **1** (side and top views; DFT calculation).[12]

sharp proton signals of **1** in CD_3CN (Fig. 2a) were characteristically broadened in D_2O/CD_3CN (Fig. 2b) in the ^{1}H NMR spectra. The significant broadening of the NMR signals of **1** in the aqueous solution is caused by the restricted motion of the multiple polyaromatic panels through efficient intramolecular, panel–panel interactions. Such NMR properties prompted us to investigate the host–guest structures mainly through UV-visible and fluorescence analyses.

Caged bulky coumarin dyes

As the first result, the open polyaromatic cavity of cage **1** could bind one molecule of disubstituted coumarin dyes **4** (X = S, O, and NH; Fig. 3a, left), which are hardly encapsulated by previous capsule **2** even under various conditions. The resultant caged dyes displayed unusual substituent-dependent emission enhancement, whereas these dyes virtually provide an isostructure and low to moderate emission abilities in aqueous solutions without **1**. When cage **1** (0.14 μmol) and benzothiazolyl-based coumarin dye **4a** (X = S; 0.41 μmol) were stirred in a 15 : 1 water/acetonitrile (AN) solution (0.45 mL) at 80 °C for 2 h, a clear pale yellow solution of 1 : 1 host–guest complex **1**·**4a** was obtained in 50% yield after filtration (Fig. 3a).[11] Rigid and hydrophobic dye **4a** itself, with a maximum length of 1.5 nm, is *insoluble* in the aqueous solution (15 : 1 water/AN) yet soluble in a 2 : 1 water/AN solution (up to 8 μM). Whereas the ^{1}H NMR spectrum of **1**·**4a** was broadened like that of empty **1** (Fig. S26† and 2b), the ESI-TOF MS and UV-visible analyses clearly indicated the 1 : 1 host–guest complex formation (Fig. S26c and S19†) and the binding of **4a** in the hydrophobic cavity of **1**, respectively. New absorption bands derived from caged **4a** were found in the range of 430 to 530 nm, which are slightly red-shifted ($\Delta\lambda$ = +9 nm) relative to the bands of uncaged **4a** in 2 : 1 water/AN (Fig. 3b). The emission bands of **4a** were also red-shifted upon binding (λ_{max} = 519 nm, $\Delta\lambda$ =

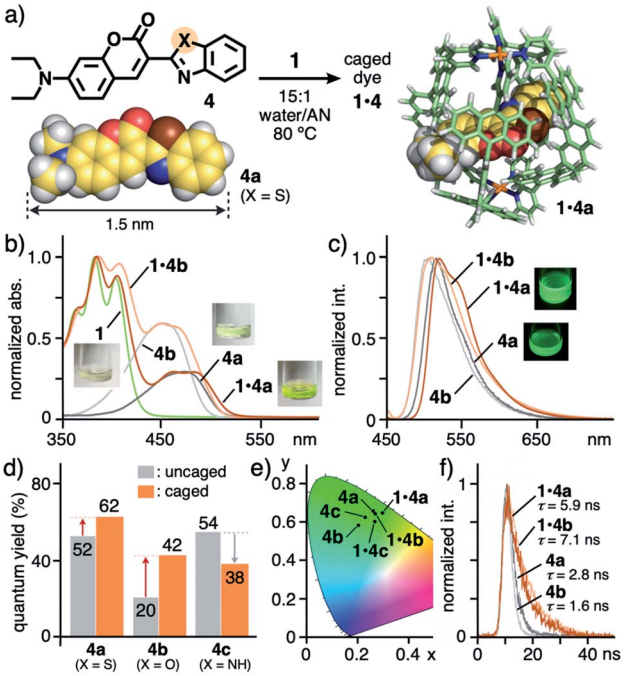

Fig. 3 (a) Formation of caged dyes **1**·**4** (X = S, O, and NH) and the optimized structures of **4a** and **1**·**4a** (R^1 = H for clarity).[11] (b) UV-visible spectra and photographs (r.t., 15 : 1 water/acetonitrile (AN)) of **1**·**4a**, **1**·**4b**, **1**, and **4a**, **4b** (in 2 : 1 water/AN), (c) their fluorescence spectra (λ_{ex} = 450 nm) and (d) quantum yields, and (e) their CIE diagram (before and after binding by **1**). (f) Fluorescence lifetimes (r.t., λ_{ex} = 355 nm, 15 : 1 or 2 : 1 water/AN) of **1**·**4a**, **1**·**4b**, and **4a**, **4b**.

+6 nm; Fig. 3c). These rather small shifts indicated the absence of host–guest π-stacking and charge-transfer (CT) interactions in the polyaromatic cavity. The host–guest structure of **1**·**4a** is stable under ambient dilution conditions (~35 μM; Fig. S19c†), implying a moderate binding constant (~2.5 × 10^4 M^{-1}).[11]

Isostructural coumarin dyes such as benzoxazolyl derivative **4b** (X = O) and benzimidazolyl derivative **4c** (X = NH) were also bound by **1** under the same conditions (Fig. 3a). New absorption and emission bands of the caged coumarins were observed in their spectra (Fig. 3b, c and S19–S21†),[11] in a manner similar to the spectroscopic properties of **4a**. Again, slight band shifts (Δλ = +3–17 nm) for **1**·**4b** and **1**·**4c** suggested the absence of host–guest π–π and CT interactions.

The solution of caged dye **1**·**4a** emitted strong green fluorescence with high quantum yield (Φ_F = 62%) in water/AN solution, upon light irradiation (λ_{ex} = 450 nm; Fig. 3d), whereas cage **1** itself shows no fluorescence despite possessing multiple anthracene fluorophores. Notably, the emission quantum yield of **4a** (Φ_F = 52%) was enhanced by 1.2-fold within **1**, in contrast to the majority of previous coordination hosts, which quench guest fluorescence to a large degree, owing to the heavy metal effect and host–guest π-stacking/CT interactions.[4,6] The emission properties of **1**·**4a** were maintained for at least 7 d at ambient temperature in the dark (Fig. S19a†).

The green emission of coumarin dyes **4b** and **4c** was further enhanced by 2.1-fold (Φ_F = 20 → 42%) yet slightly suppressed (Φ_F = 54 → 38%), respectively, within the cage (Fig. 3d).[11] The CIE diagram displayed a minor change of the emission colors of the dyes within the cage, due to weak host–guest steric and electronic interactions (Fig. 3e). The fluorescence lifetime (τ) of **1**·**4a** was estimated to be 5.9 ns, which is longer than that of free **4a** (τ = 2.8 ns; Fig. 3f), indicating the stabilization of the excited state upon caging. Further prolongation of the guest emission lifetime was observed for **1**·**4b** (τ = 7.1 ns) under the same conditions. The opposite emission behavior of **4c** is likely derived from a weakening of the intramolecular hydrogen-bonding interaction between the C=O and N–H (Fig. S27b†).

The optimized structure of caged dye **1**·**4a** indicated that the rod-shaped dye is threaded through the opposite two windows of the host framework (Fig. 3a, right). Importantly, no aromatic–aromatic stack between the host and guest frameworks is observed, consistent with small band shifts in the UV-visible and fluorescence spectra and the high quantum yield. The coumarin core can be effectively isolated from aqueous solvent, acting as an emission-quenching medium, by the polyaromatic shell. The bulky aromatic substituent of **4a** is situated at the window with close host–guest contact, which most probably alters the guest emission in the cavity, depending on the difference in the heteroatom (*i.e.*, S, O, and NH).

Caged bulky perylene bisimide dyes

Next, perylene bisimide (PBI) dyes **5** with two substituted aromatic rings were employed as longer and more rigid organic dyes (2.2 nm in maximum length) than **4**. Although the binding of these bulky dyes by synthetic hosts has been quite uncommon,[13,14] one molecule of **5** was selectively trapped by the open framework of **1** in a threading fashion like **4**, accompanying a unique change in color. The sonication (40 kHz, 20 min) of a mixture of cage **1** and 2,6-diisopropylphenyl-based PBI dye **5a** (0.14 μmol each) in 5 : 1 water/AN (1.0 mL) gave rise to a red clear solution of 1 : 1 host–guest complex **1**·**5a** in 48% yield, through removal of suspended free **5a** *via* simple filtration (Fig. 4a).[11] The broad ^{1}H NMR spectrum of the red solution at room temperature partially became sharp at elevated temperature (*e.g.*, 75 °C). The host aromatic signals were split complicatedly and the guest signal H_A was observed at −0.96 ppm with a large upfield shift (Δδ = −2.2 ppm; Fig. 4b–d), due to the desymmetrization and aromatic shielding effect of the host framework, respectively. The 1 : 1 host–guest complexation was confirmed by the ESI-TOF MS analysis, which showed molecular ion peaks corresponding to the $[\mathbf{1}\cdot\mathbf{5a} - n\cdot NO_3^-]^{n+}$ (n = 4 and 3) species (Fig. 4e). Owing to the very broad DOSY spectrum of **1**·**5a** at room temperature, the product size was determined by the DLS analysis (d = 4.3 nm; Fig. S32c†).[11]

In the same way, caged dyes **1**·**5b** and **1**·**5c** were obtained by the treatment of cage **1** with 2,5-di(*tert*-butyl)phenyl-based PBI **5b** and 3,5-dimethylphenyl-based PBI **5c**, respectively (Fig. S28a†).[11] Although no host–guest titration studies were performed due to the insolubility of **5a–c** in 5 : 1 water/AN without **1**, the concentration-dependent UV-visible analysis of **1**·**5a** revealed the stability of the host-complex at ~3.5 μM (Fig. S28c†), suggesting a binding constant of >10^8 M^{-1}.[11] Again,

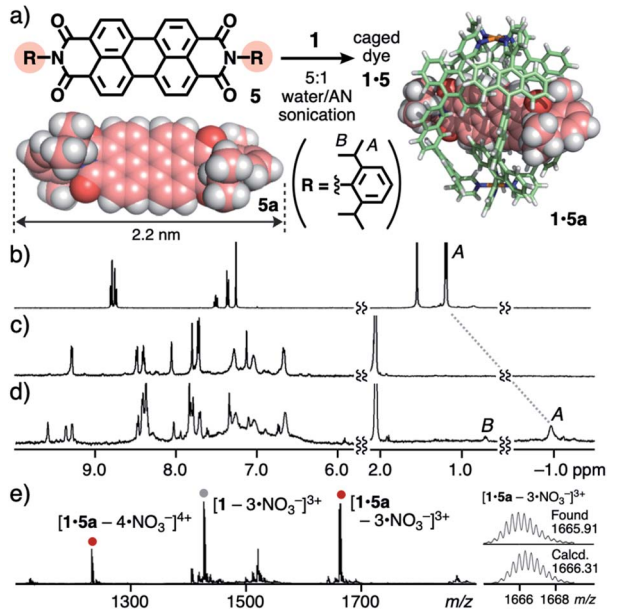

Fig. 4 (a) Formation of caged dye **1·5** and the optimized structures of **5a** and **1·5a** (R^1 = H for clarity).[11] ^{1}H NMR spectra (500 MHz, 5 : 1 D_2O/CD_3CN, 75 °C) of (b) **5a** (in $CDCl_3$, r.t.), (c) **1**, and (d) **1·5a**. (e) ESI-TOF MS spectrum (5 : 1 water/AN) of **1·5a**.

no encapsulation of bulky PBIs **5a–c** took place with capsule **2** even under various conditions, owing to its closed cavity.

Drastic color change of diisopropylphenyl derivative **5a** from yellow to red through binding by **1** was observed and the present unusual phenomenon was elucidated by theoretical spectroscopic studies. Monomeric free **5a** is yellow in less polar solvent (*e.g.*, CH_2Cl_2; Fig. 5a) and orange in polar solvent (*e.g.*, DMSO; Fig. S28b†) with similarly shaped absorption bands.[11] In sharp contrast, caged dye **1·5a** displayed red color in aqueous solution. The visible difference was qualified by UV-visible and fluorescence analyses. The relatively sharp absorption bands of uncaged **5a** were recorded in CH_2Cl_2 in the range of 420 to 550 nm, which were significantly broadened and red-shifted (up to ~610 nm) within **1** (Fig. 5a). The emission band of caged **5a** was further broadened and shifted (λ_{max} = 625 nm, $\Delta\lambda$ = +78 nm) relative to free **5a** (Fig. 5b). A similar yellow-to-red color change was observed for bulky di(*tert*-butyl)phenyl derivative **5b**. The sharp absorption bands (415–550 nm) of **5b** in CH_2Cl_2 were largely broadened and red-shifted (up to ~600 nm) through caging in aqueous solution (Fig. 5c).

In contrast, neither color change nor spectral change occurred for less bulky and planar dimethylphenyl derivative **5c**, featuring broad absorption bands at 430–600 nm (Fig. 5c), through binding by **1** under the same conditions. The absorption bands derived from **1** at 330–430 nm remained also unchanged upon caging. These results suggest that no donor–acceptor π-stacking interactions exist between the cage cavity and the PBI framework of **5a–c**.

The theoretical studies indicated that the observed band shifts and broadening stem from the twisted conformation between the bulky substituents (R) and the PBI core of dye **5** within cage **1**.[15] The dihedral angle (ϕ) about the phenyl and imide rings of **5** corresponds to its electronic absorption features. For instance, the most stable conformer **5a** with ϕ = 90° theoretically provides an intense, single electronic absorption band at 500 nm (Fig. 5d). The band is red-shifted by +6 nm through its transformation into one of the metastable conformers with ϕ = 70°. The estimated energy is +75 kJ mol^{-1} higher than that of the most stable conformer. In the optimized host–guest structure of **1·5a**, dye **5a** displayed ϕ = 70° within **1** (Fig. 4a, right). Accordingly, the observed, unusual color changes of caged **5a** and **5b** were induced through non-covalent twisting of the bulky substituents in the open cavity.

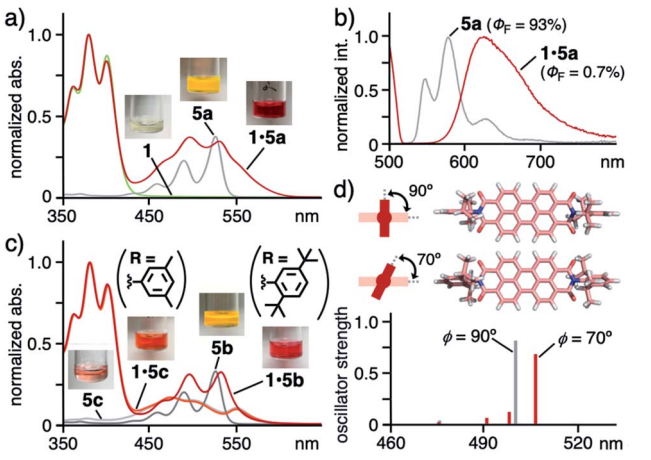

Fig. 5 (a) UV-visible spectra and photographs (5 : 1 water/AN, r.t.) of **1·5a**, **1**, and **5a** (in CH_2Cl_2) and (b) their fluorescence spectra (λ_{ex} = 500 nm) except for **1**. (c) UV-visible spectra (5 : 1 water/AN, r.t.) of **1·5b**, **1·5c**, **5b** (in CH_2Cl_2) and **5c** (in DMSO). (d) Optimized structures of **5a** with ϕ = 90° and 70° and their predicted, electronic absorption bands.[15]

Caged bulky porphyrin dyes

Finally, to our surprise, the open polyaromatic cavity enabled cage **1** to bind one molecule of porphyrin dyes **6** bearing four or eight substituents. The encapsulation of porphyrins and metalloporphyrins by large proteins has been intensively studied so far[16] yet a non-biological approach using coordination cages and capsules is complicated by the large and bulky dye frameworks.[5] In a manner similar to **5**, tetraphenylporphyrin **6a** (R = Ph; 1.8 nm in maximum length) in purple was bound by **1** *via* sonication (40 kHz) of the mixture in 8 : 1 water/AN for 20 min (Fig. 6a).[11] The resultant brown solution including 1 : 1 host–guest complex **1·6a** (70% yield) exhibited new absorption bands, assignable to caged **6a** in the UV-visible spectrum (Fig. 6b). The characteristic Soret and the first Q bands of **6a** were red-shifted by +3 and +4 nm, respectively, as compared with those of free **6a** in CH_2Cl_2, through the binding. These bands remained unchanged even after 7 d under ambient conditions, suggesting adequate stability of the host–guest structure (Fig. S37a†). The insolubility of dye **6a** in aqueous solution prevented titration, but concentration-dependent UV-visible analysis of **1·6a** in 8 : 1 water/AN indicated high

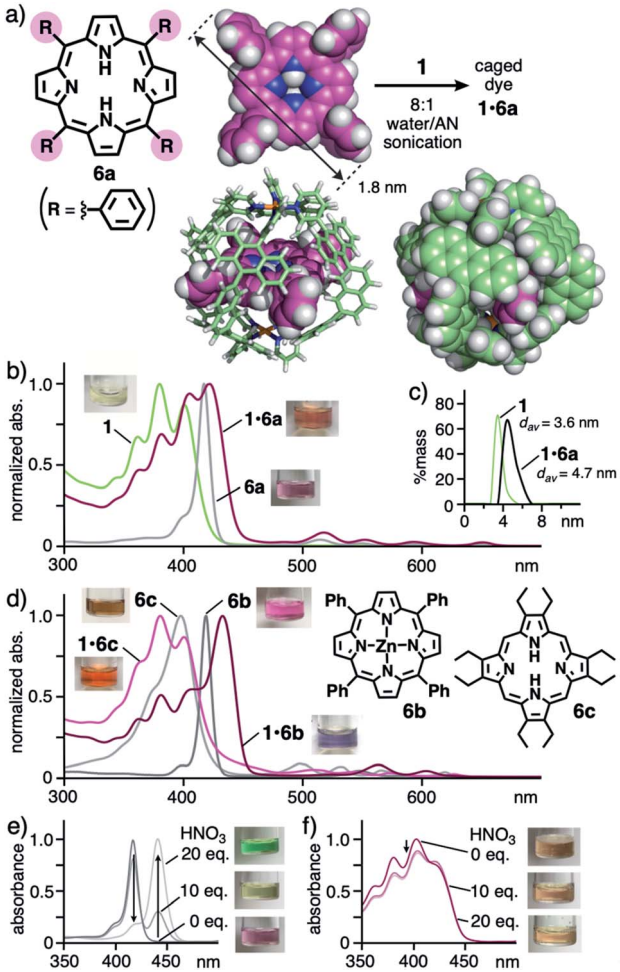

Fig. 6 (a) Formation of caged dye **1·6a** and the optimized structures of **6a** and **1·6a** (R^1 = H for clarity).[11] (b) UV-visible spectra and photographs (8 : 1 water/AN, r.t.) of **1·6a**, **1**, and **6a** (in CH_2Cl_2) and (c) their DLS charts (r.t.) except for **6a**. (d) UV-visible spectra and photographs (8 : 1 water/AN, r.t.) of **1·6b**, **1·6c**, and **6b**, **6c** (in CH_2Cl_2). UV-visible spectra and photographs (r.t.) of (e) **6a** in CH_2Cl_2 and (f) **1·6a** in 8 : 1 water/AN, after addition of HNO_3 (0–20 equivalents).

stability ($K_a > 10^8$ M^{-1}) against high dilution (up to ~3.5 μM; Fig. S39c†).[11] In the ^{1}H NMR and ESI-TOF MS spectra of the resultant solution, the guest and host–guest signals were scarcely observed owing to significant signal broadening and instability under MS conditions (*e.g.*, extremely low concentration and high vacuum), respectively (Fig. S39†).[11] The DLS analysis supported the product size with a single peak at d = 4.7 nm, slightly larger than that of empty **1** (d = 3.6 nm, Fig. 6c). Unfortunately, no crystals of the host–guest complex were obtained even under various conditions.

The structure of obtained, caged dye **1·6a** was further supported by the theoretical calculation, where the four bulky substituents of **6a** are located at the four openings of **1**, whereas the large π-conjugated core of **6a** is effectively surrounded by the polyaromatic cage-like framework of **1** without direct contacts (Fig. 6a, right). The complimentary symmetry facilitates the formation of unusual host–guest complex **1·6a**. Because of the absence of host–guest π-stacking interactions in the optimized structure, the observed red-shifts of caged **6a** are most probably derived from the stabilization of its planar conformation over its butterfly-shaped one[16] within **1**.

Other bulky porphyrin dyes were also trapped by cage **1** in aqueous solution with selectivity[17] and the caged dyes were protected by the polyaromatic frameworks against acid. Further color and absorption changes were found through caging of Zn(II)-tetraphenylporphyrin **6b** by **1** through the same sonication protocol. Although **6b** itself shows no solvatochromic properties, the resultant solution of **1·6b** is bluish-purple in contrast to a pink solution of free **6b** in CH_2Cl_2 (Fig. 6d). In addition, distinct shifts of the Soret and first Q bands of **6b** by approximately +15 nm in each case were observed in the UV-visible spectrum upon trapping. These unusual shifts are most likely derived from the cage-directed, non-covalent planarization of the metalloporphyrin framework. Caged octaethylporphyrin dye **1·6c** and tetrakis(pentafluorophenyl) porphyrin dye **1·6d** also displayed modulated color and altered absorption bands, relative to the corresponding free dyes (Fig. 6d and S37b†). Furthermore, the polyaromatic cage-like framework of **1** could prevent the π-conjugated core of **6a** from protonation under acidic conditions. Uncaged **6a** was fully protonated upon addition of 20 equivalent of HNO_3, accompanying its color and spectral changes (Fig. 6e).[18] On the other hand, the color and spectrum of caged **6a** remained intact, except for a slight intensity change, even after the addition of excess HNO_3 (up to 100 equivalent; Fig. 6f and S41a†).[11] The present protection effect for the porphyrin dye, which was also found for **1·6c** (Fig. S41b†), has not been reported with the previous synthetic hosts, except for a covalent cage from the Stoddart group.[5,19] The theoretical studies indicated that the host–guest complexation of **1** and diprotonated dye **6a**′ is unfavorable (ΔE > 800 kJ mol^{-1} based on PM6 calculation; Table S2†), owing to its sterically demanding, largely distorted framework, rather than long-range, host–guest cation–cation repulsion (d = 0.7 nm; Fig. S43†).[11]

Conclusions

We have demonstrated the binding and spectroscopic modulation of three types of bulky organic dyes (≥1.5 nm in maximum length) by a polyaromatic cage in aqueous solution. Binding dyes with several bulky substitutes has faced many difficulties so far, because neither too large nor too small cavities/windows are suitable for the desired host compounds. We herein employed an M_2L_4 cage with an open polyaromatic cavity, after simple modification of its hydrophilic side-chains, to successfully bind sterically demanding dyes with coumarin, perylene bisimide, and porphyrin cores. Thanks to size and shape host–guest matching as well as effective host–guest interactions (*i.e.*, hydrophobic effect and multiple CH–π interactions), these dyes were straightforwardly caught by the cage in a threading fashion. Notably, the caged dyes displayed unusual fluorescence/color and spectroscopic features due to the polyaromatic cage effect, without π-stacking interactions, which was revealed by detailed theoretical and spectroscopic studies.

As compared with typical covalent functionalization and previous host–guest systems targeting small and less bulky dyes, the present non-covalent modification of large and bulky organic dyes provides various advantages, since the coordination framework can for example be easily modulated *via* doping with heteroatoms and attachment of interactive side chains. Biological and materials applications of the present and other caged bulky dyes will be our next research targets.

Data availability

The experimental procedures and analytical data are available in the ESI.†

Author contributions

M. U., N. K., L. C., and M. Y. designed the work, carried out research, analyzed data, and wrote the paper. M. Y. is the principal investigator. All authors discussed the results and commented on the manuscript.

Conflicts of interest

There are no conflicts to declare.

Acknowledgements

This work was supported by JSPS KAKENHI (Grant No. JP20K22552/JP21K18951/JP22H00348/JP22H0556), AMED (Grant No. H421TS), and The Mitsubishi Foundation (Research Grants in the Natural Sciences).

Notes and references

1 (*a*) M. Daniel, S. D. Bhattacharya, A. Arya and V. M. Raole, *Natural Dyes: Scope and Challenges*, Scientific Publishers, Jodhpur, 2006; (*b*) *Industrial Dyes: Chemistry, Properties, Applications*, ed. K. Hunger, Wiley-VCH, 2002.

2 (*a*) F. Würthner, C. R. Saha-Möller, B. Fimmel, S. Ogi, P. Leowanawat and D. Schmidt, *Chem. Rev.*, 2016, **116**, 962–1052; (*b*) D. Cao, Z. Liu, P. Verwilst, S. Koo, P. Jangjili, J. S. Kim and W. Lin, *Chem. Rev.*, 2019, **119**, 10403–10519; (*c*) C. J. Kingsbury and M. O. Senge, *Coord. Chem. Rev.*, 2021, **431**, 213760.

3 R. N. Dsouza, U. Pischel and W. M. Nau, *Chem. Rev.*, 2011, **111**, 7941–7980.

4 Recent reviews on coordination cages: (*a*) T. R. Cook and P. J. Stang, *Chem. Rev.*, 2015, **115**, 7001–7045; (*b*) C. J. Brown, F. D. Toste, R. G. Bergman and K. N. Raymond, *Chem. Rev.*, 2015, **115**, 3012–3035; (*c*) L.-J. Chen, H.-B. Yang and M. Shionoya, *Chem. Soc. Rev.*, 2017, **46**, 2555–2576; (*d*) I. Sinha and P. S. Mukherjee, *Inorg. Chem.*, 2018, **57**, 4205–4221; (*e*) F. J. Rizzuto, L. K. S. von Krbek and J. R. Nitschke, *Nat. Rev. Chem.*, 2019, **3**, 204–222; (*f*) A. B. Grommet, M. Feller and R. Klajn, *Nat. Nanotechnol.*, 2020, **15**, 256–271; (*g*) E. G. Percástegui, T. K. Ronson and J. R. Nitschke, *Chem. Rev.*, 2020, **120**, 13480–13544; (*h*) H. Takezawa and M. Fujita, *Bull. Chem. Soc. Jpn.*, 2021, **94**, 2351–2369; (*i*) S. Pullen, J. Tessarolo and G. H. Clever, *Chem. Sci.*, 2021, **12**, 7269–7293.

5 Binding of bulky porphyrin dyes *via coordination bonds*: (*a*) M. L. Merlau, M. del P. Mejia, S. T. Nguyen and J. T. Hupp, *Angew. Chem., Int. Ed.*, 2001, **40**, 4239–4242; (*b*) M. Otte, P. F. Kuijpers, O. Troeppner, I. Ivanović-Burmazović, J. N. H. Reek and B. de Bruin, *Chem.–Eur. J.*, 2013, **19**, 10170–10178; (*c*) F. J. Rizzuto, W. J. Ramsay and J. R. Nitschke, *J. Am. Chem. Soc.*, 2018, **140**, 11502–11509.

6 (*a*) M. Yoshizawa and J. K. Klosterman, *Chem. Soc. Rev.*, 2014, **43**, 1885–1898; (*b*) M. Yoshizawa and M. Yamashina, *Chem. Lett.*, 2017, **46**, 163–171; (*c*) M. Yoshizawa and L. Catti, *Acc. Chem. Res.*, 2019, **52**, 2392–2404; (*d*) L. Catti, R. Sumida and M. Yoshizawa, *Coord. Chem. Rev.*, 2022, **460**, 214460.

7 Other polyaromatic capsules and tubes: (*a*) K. Kondo, J. K. Klosterman and M. Yoshizawa, *Chem.–Eur. J.*, 2017, **23**, 16710–16721; (*b*) K. Yazaki, L. Catti and M. Yoshizawa, *Chem. Commun.*, 2018, **54**, 3195–3206.

8 (*a*) N. Kishi, Z. Li, K. Yoza, M. Akita and M. Yoshizawa, *J. Am. Chem. Soc.*, 2011, **133**, 11438–11441; (*b*) M. Yamashina, Y. Sei, M. Akita and M. Yoshizawa, *Nat. Commun.*, 2014, **5**, 4662.

9 Multiple host–guest interactions supported by X-ray crystallographic analysis: (*a*) K. Yazaki, M. Akita, S. Prusty, D. K. Chand, T. Kikuchi, H. Sato and M. Yoshizawa, *Nat. Commun.*, 2017, **8**, 15914; (*b*) S. Kusaba, M. Yamashina, M. Akita, T. Kikuchi and M. Yoshizawa, *Angew. Chem., Int. Ed.*, 2018, **57**, 3706–3710; (*c*) M. Yamashina, S. Kusaba, M. Akita, T. Kikuchi and M. Yoshizawa, *Nat. Commun.*, 2018, **9**, 4227; (*d*) M. Yamashina, T. Tsutsui, Y. Sei, M. Akita and M. Yoshizawa, *Sci. Adv.*, 2019, **5**, eaav3179; (*e*) N. Kishida, K. Matsumoto, Y. Tanaka, M. Akita, H. Sakurai and M. Yoshizawa, *J. Am. Chem. Soc.*, 2020, **142**, 9599–9603; (*f*) R. Sumida, Y. Tanaka, K. Niki, Y. Sei, S. Toyota and M. Yoshizawa, *Chem. Sci.*, 2021, **12**, 9946–9951.

10 M. Yamashina, T. Yuki, Y. Sei, M. Akita and M. Yoshizawa, *Chem. Eur. J.*, 2015, **21**, 4200–4204.

11 See the ESI.† The yields of the resultant host–guest complexes (uptake ratios) were estimated by UV-visible analysis (with a calibration curve method) in organic solvent (*i.e.*, DMSO), after the removal of suspended unbound dyes by filtration and the lyophilization of the aqueous solutions of cage **1** and its host–guest complexes. The geometry optimizations of host–guest complexes were performed with molecular mechanics calculations (forcite module, BIOVIA Materials Studio 2020, version 20.1.0.5).

12 ^{1}H DOSY NMR spectrum showed the presence of a single product with a diffusion coefficient (D) of 4.68×10^{-10} m^2 s^{-1} (Fig. S14†). The optimized structure of **1** was obtained by DFT calculation (CAM-B3LYP/LanL2DZ (for Pt), 6-31G(d,p) (for organic atoms) level of theory).

13 Binding of PBI dyes with *hydrophilic side chains* by covalent hosts: (*a*) F. Biedermann, E. Elmalem, I. Ghosh, W. M. Nau and O. A. Scherman, *Angew. Chem., Int. Ed.*, 2012, **51**, 7739–7743; (*b*) W. Liu, S. Bobbala, C. L. Stern,

J. E. Hornick, Y. Liu, A. E. Enciso, E. A. Scott and J. F. Stoddart, *J. Am. Chem. Soc.*, 2020, **142**, 3165–3173.

14 Encapsulation of multiple PBI dyes in a stacked fashion: K. Ito, T. Nishioka, M. Akita, A. Kuzume, K. Yamamoto and M. Yoshizawa, *Chem. Sci.*, 2020, **11**, 6752–6757.

15 The optimized structure of **5a** ($\phi = 90°$) was obtained by DFT calculation (CAM-B3LYP/6-31G(d,p) level of theory). The predicted absorption bands were obtained by TD-DFT calculation (B3LYP/6-31G(d) level of theory; Fig. 5d and S35a†). Additional calculations of **5a** including dispersion effects were examined using DFT (CAM-B3LYP+D3BJ/6-31G(d,p) level of theory) and TD-DFT (B3LYP+D3BJ/6-31G(d) level of theory; Fig. S35b†).[11]

16 T. L. Poulos, *Chem. Rev.*, 2014, **114**, 3919–3962.

17 The incorporation efficiency of cage **1** depends on the substituents on the porphyrin core.[11] Competitive binding experiments revealed that **1** selectively binds **6a** (>80% selectivity) from a mixture of **6a** and octaethylporphyrin (**6c**), due to steric effects (Fig. S45†). More rigid **6b** (∼30% selectivity) was inferior to **6a** regarding the incorporation by **1** (Fig. S45†).

18 O. Finikova, A. Galkin, V. Rozhkov, M. Cordero, C. Hägerhäll and S. Vinogradov, *J. Am. Chem. Soc.*, 2003, **125**, 4882–4893.

19 W. Liu, C. Lin, J. A. Weber, C. L. Stern, R. M. Young, M. R. Wasielewski and J. F. Stoddart, *J. Am. Chem. Soc.*, 2020, **142**, 8938–8945.